Electronic Supplementary Information

Adsorption of HCN on cosmic silicates: a periodic quantum mechanical study

Niccolò Bancone[1,2], Stefano Pantaleone[1], Piero Ugliengo[1], Albert Rimola[2] and Marta Corno[1*]*

[1]Dipartimento di Chimica and NIS – Nanostructured Interfaces and Surfaces – Centre, Università degli Studi di Torino, via P. Giuria 7, 10125, Torino, Italy

[2]Departament de Química, Universitat Autònoma de Barcelona, 08193 Bellaterra, Spain

*Corresponding authors: marta.corno@unito.it, telephone: +390116702439
albert.rimola@uab.cat, telephone:+34935812164

Computational Details

Basis set

Here follow the adopted basis sets for forsterite atoms (Mg, O, Si, taken by Bruno's)[1] and the polarized Ahlrichs-VTZ[2] for HCN atoms (CRYSTAL17 format):

Mg

```
12 5
 0 0 8 2.0 1.0
  68371.8750000          0.0002226
   9699.3400900          0.0018982
   2041.1767860          0.0110451
    529.8629060          0.0500627
    159.1860000          0.1691230
     54.6848000          0.3670310
     21.2357000          0.4004100
      8.7460400          0.1498700
 0 1 5 8.0 1.0
    156.7950000          -0.0062400          0.0077200
     31.0339000          -0.0788200          0.0642700
      9.6453000          -0.0799200          0.2104000
      3.7109000          0.2906300           0.3431400
      1.6116400          0.5716400           0.3735000
 0 1 1 2.0 1.0
```

```
      0.6800000            1.0000000            1.0000000
 0 1 1 0.0 1.0
      0.2245160            1.0000000            1.0000000
 0 3 1 0.0  1.0
      0.5000000            1.0000000
```

Si

```
 14  6
 0 0 8 2.0 1.0
  87645.8000000            0.0002370
  12851.8000000            0.0019200
   2786.2800000            0.0109000
    728.0430000            0.0496000
    219.5160000            0.1668000
     75.9006000            0.3630000
     29.4602000            0.4051000
     11.9891000            0.1504000
 0 1 6 8.0 1.0
    165.9580000           -0.0088400            0.0090900
     39.3727000           -0.0859000            0.0601000
     12.7112000           -0.0712000            0.1952000
      4.7177000            0.4147000            0.3384000
      1.8482000            0.6168000            0.3006000
      0.7365000            0.1154000            0.0648000
 0 1 3 4.0 1.0
      4.1752000           -0.0199000           -0.0087000
      1.4472000           -0.1864000           -0.0043800
      0.5023000            0.0967000            0.2207000
 0 1 1 0.0 1.0
      0.3220000            1.0000000            1.0000000
 0 1 1 0.0 1.0
      0.1300000            1.0000000            1.0000000
 0 3 1 0.0 1.0
      0.6000000            1.0000000
```

O

```
 8  5
 0 0 8 2. 1.
 8020.        0.00108
 1338.        0.00804
  255.4       0.05324
   69.22      0.1681
   23.90      0.3581
    9.264     0.3855
    3.851     0.1468
    1.212     0.0728
```

```
 0 1 4 6. 1.
   49.43      -0.00883    0.00958
   10.47      -0.0915     0.0696
    3.235     -0.0402     0.2065
    1.217      0.379      0.347
 0 1 1 0.0 1.0
     0.59       1.          1.
 0 1 1 0. 1.
     0.250588 1. 1.
 0 3 1 0. 1.
    0.500     1.
```

H

```
1  4
0 0 3 1.0 1.00
     34.0613410             0.60251978E-02
      5.1235746             0.45021094E-01
      1.1646626             0.20189726
0 0 1 0. 1.00
      0.32723041            1.0000000
0 0 1 0. 1.00
      0.10307241            1.0000000
0 2 1 0. 1.
      0.8                 1.0000000
```

C

```
6 10
0 0 5 2.0 1.0
  8506.0384000   0.53373664E-03
  1275.7329000   0.41250232E-02
   290.3118700   0.21171337E-01
    82.0562000   0.82417860E-01
    26.4796410   0.24012858
0 0 1 2.0 1.0
     9.2414585   1.0000000
0 0 1 0.0 1.0
     3.3643530   1.0000000
0 0 1 0.0 1.0
     0.87174164  1.0000000
0 0 1 0.0 1.0
     0.36352352  1.0000000
0 0 1 0.0 1.0
     0.12873135  1.0000000
0 2 4 2.0 1.0
    34.7094960   0.53300974E-02
```

```
     7.9590883    0.35865814E-01
     2.3786972    0.14200299
     0.81540065   0.34203105
0 2 1 0.0 1.0
     0.28953785   1.0000000
0 2 1 0.0 1.0
     0.10084754   1.0000000
0 3 1 0.0 1.0
   0.8000000    1.0000000


N

7 10
0 0 5 2.0 1.00
   11913.4167560            -0.52297017365E-03
    1786.7213834            -0.40428404036E-02
     406.59012834           -0.20772715125E-01
     114.92525065           -0.81183137849E-01
      37.105883422          -0.23871497395
0 0 1 2.0 1.00
      12.971676198           1.0000000
0 0 1 0.0 1.00
       4.7302291164          1.0000000
0 0 1 0.0 1.00
       1.2525184258          1.0000000
0 0 1 0.0 1.00
       0.51260071231         1.0000000
0 0 1 0.0 1.00
       0.17939714002         1.0000000
0 2 4 3.0 1.00
      49.218758392           0.55526953476E-02
      11.348935304           0.38054617957E-01
       3.4285088246          0.14941412242
       1.1799512559          0.34898187368
0 2   1 0.0 1.00
       0.41726122577         1.0000000
0 2   1 0.0 1.00
       0.14295131280         1.0000000
0 3 1 0.0 1.00
       1.0000000             1.0000000
```

Results

HCN adducts on forsterite surfaces

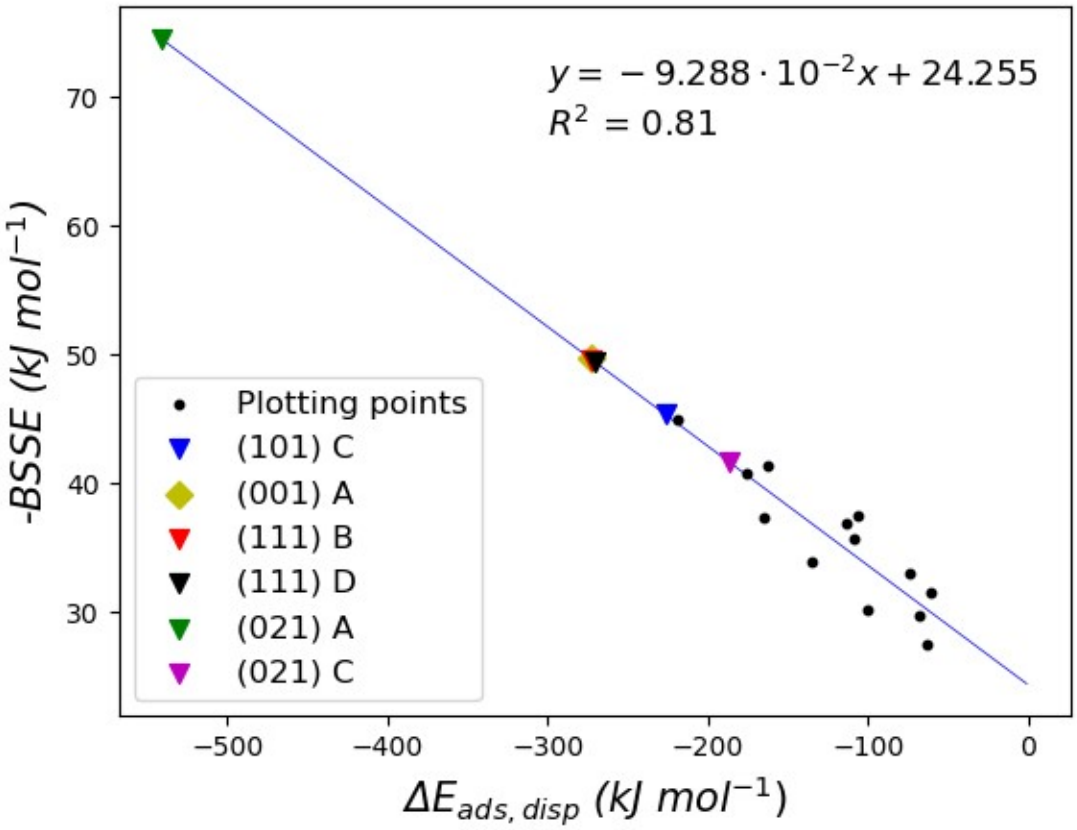

Figure S1. Linear dependence between $\Delta E_{ads,disp}$ and corresponding BBSE values. The interpolated points represent the structures for which the CP method was not feasible.

Here follow all the structures of the studied HCN adducts on forsterite surfaces

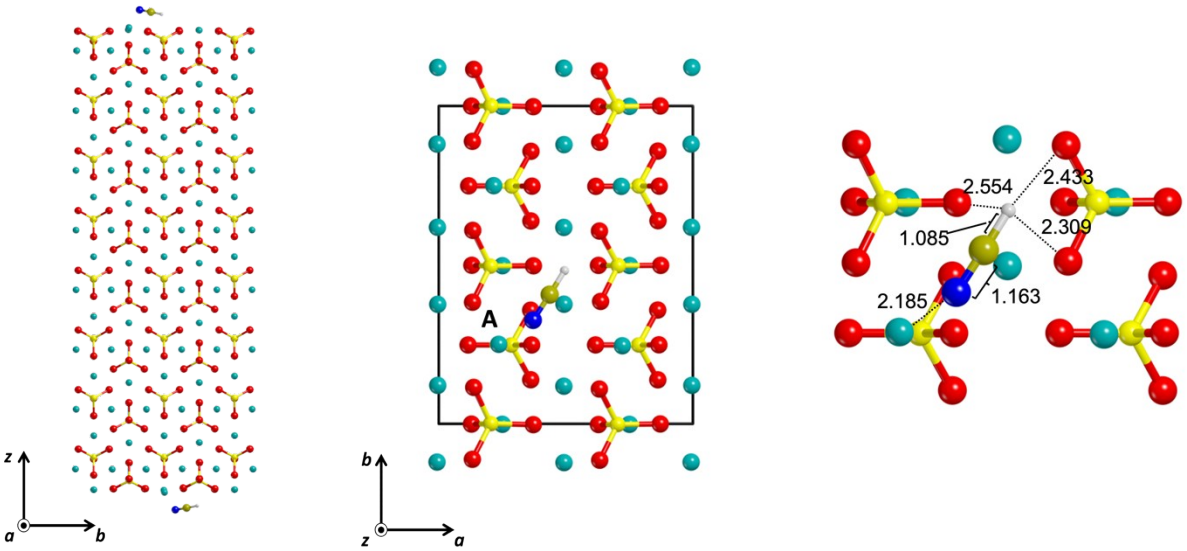

Figure S2. Side and top views of the (010) A structure.

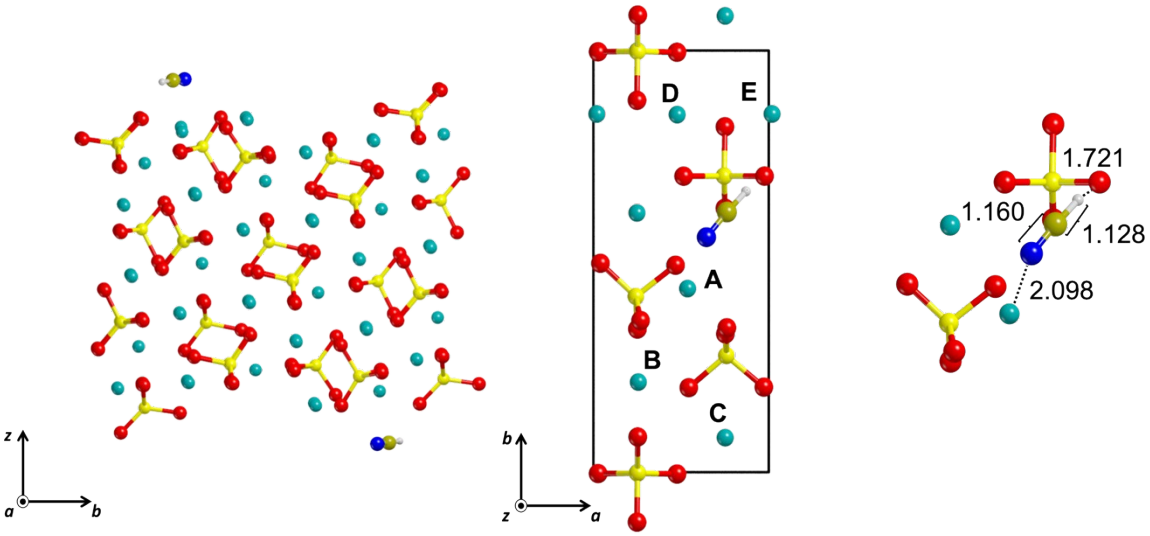

Figure S3. Side and top views of the (120) A structure.

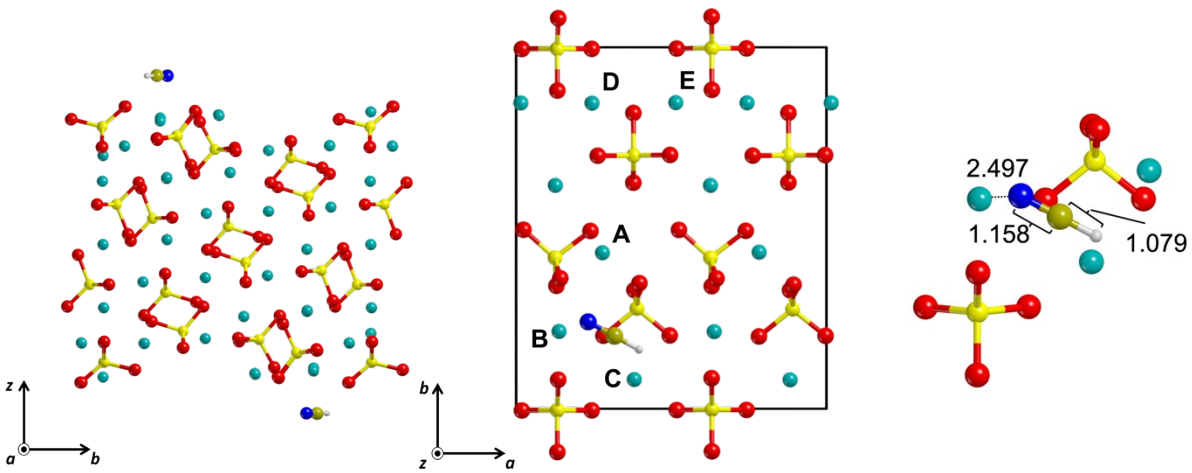

Figure S4. Side and top views of the (120) B structure.

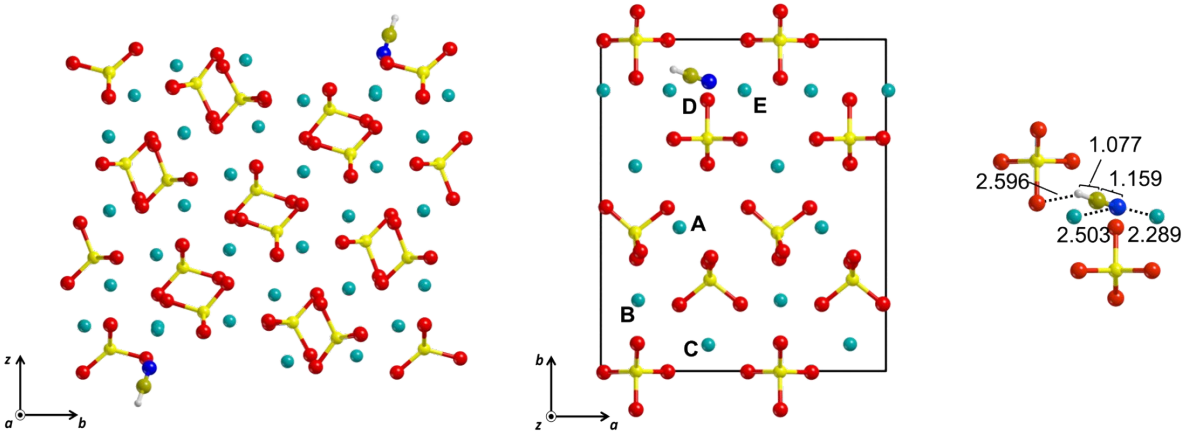

Figure S5. Side and top views of the (120) C structure. After initially placing the molecule on the C site, it displaced towards the D and E sites during the geometry optimization. The same structure was obtained by placing the HCN molecule on D and E sites.

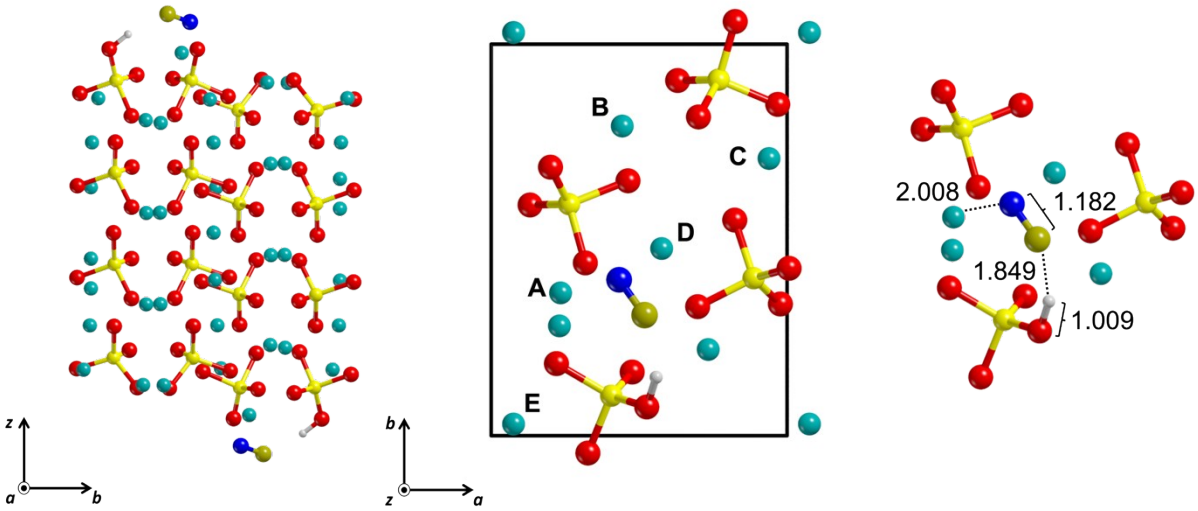

Figure S6. Side and top views of the (101) A structure. The same structure was obtained by placing the HCN molecule on the D site.

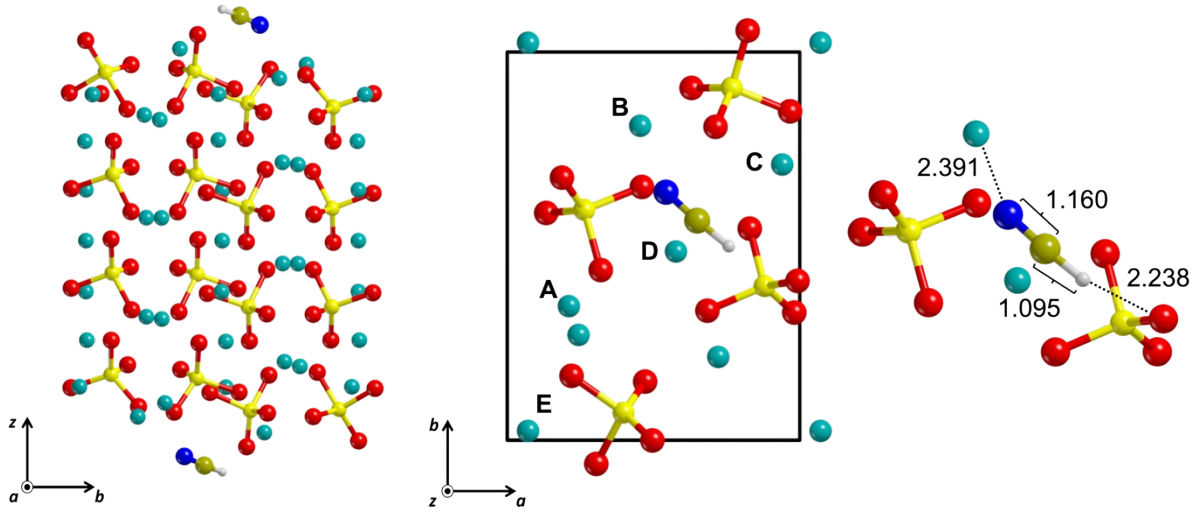

Figure S7. Side and top views of the (101) B structure.

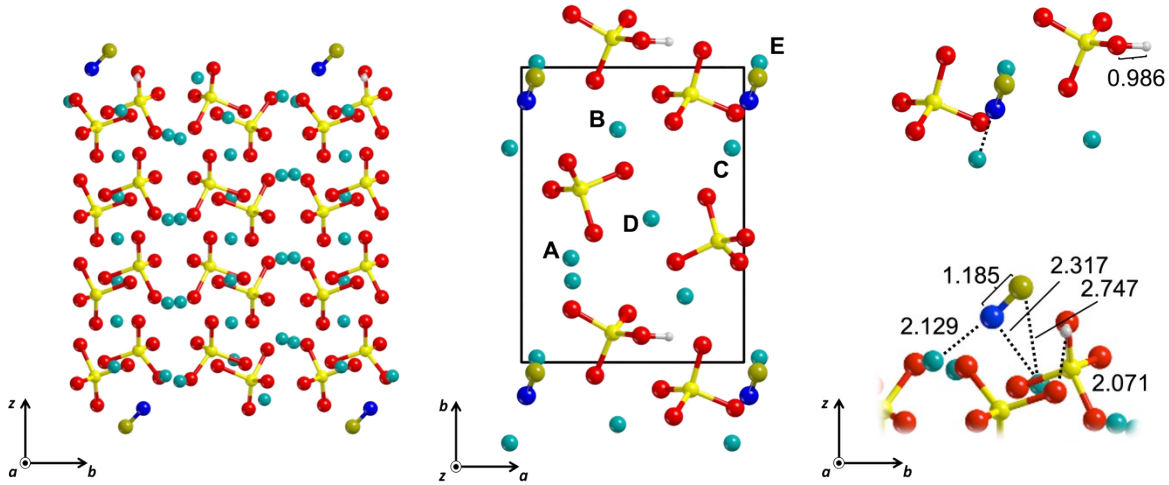

Figure S8. Side and top views of the (101) C structure. The same structure was obtained by placing the HCN molecule on the E site.

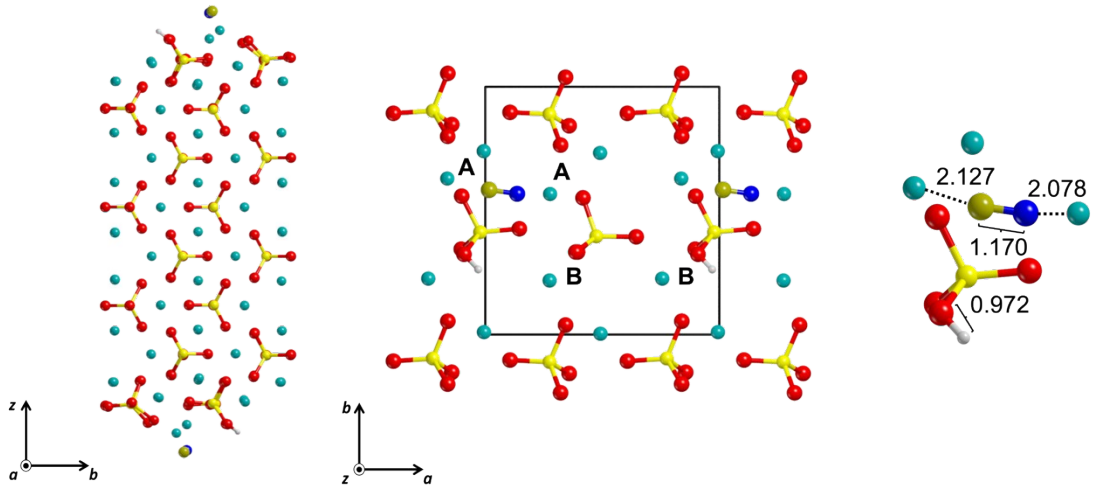

Figure S9. Side and top views of the (001) A structure.

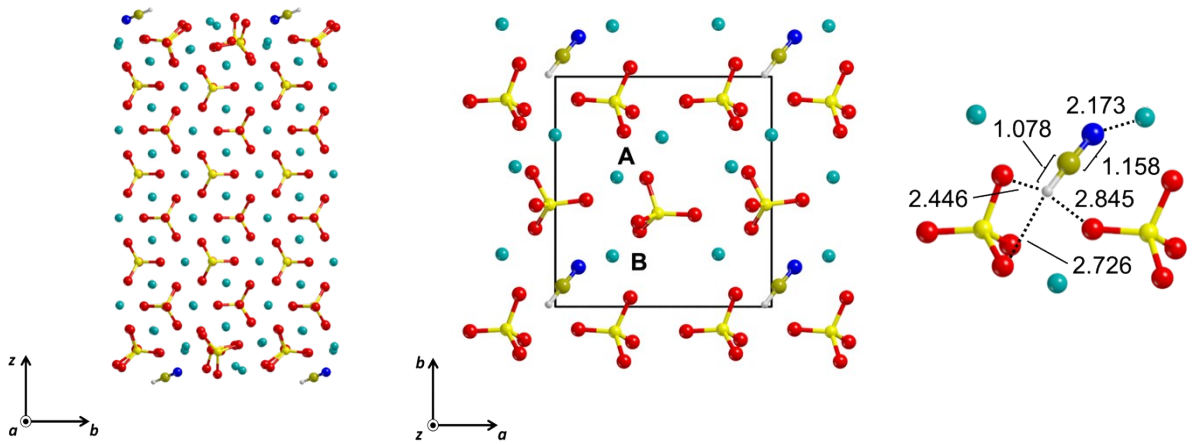

Figure S10. Side and top views of the (001) B structure.

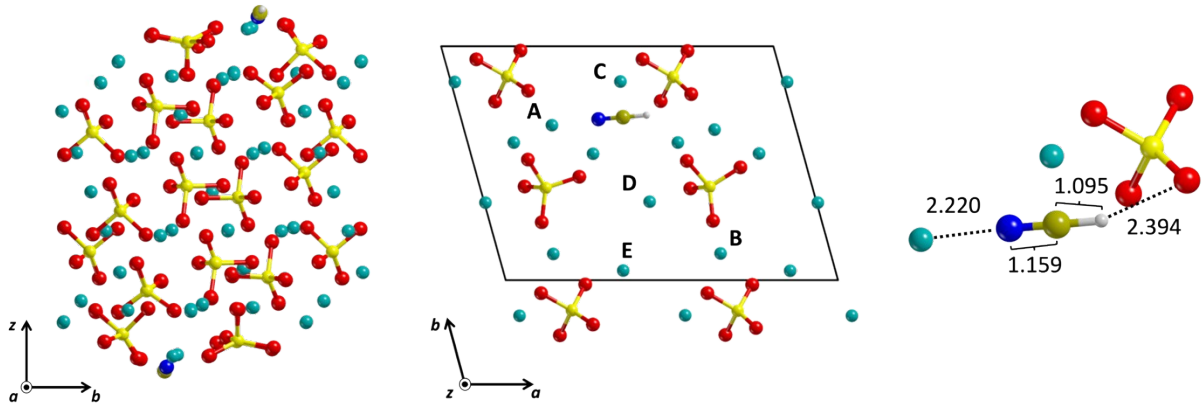

Figure S11. Side and top views of the (111) A structure.

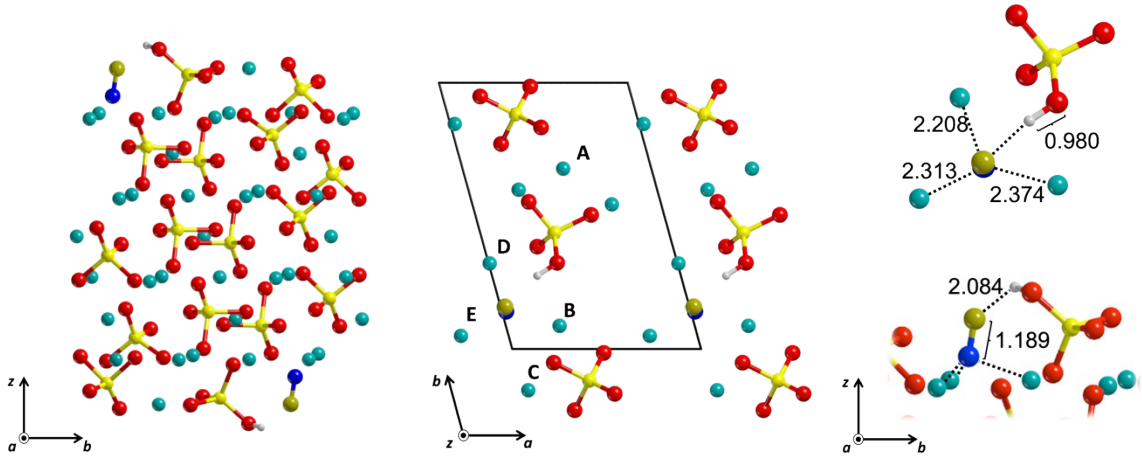

Figure S12. Side and top views of the (111) B structure.

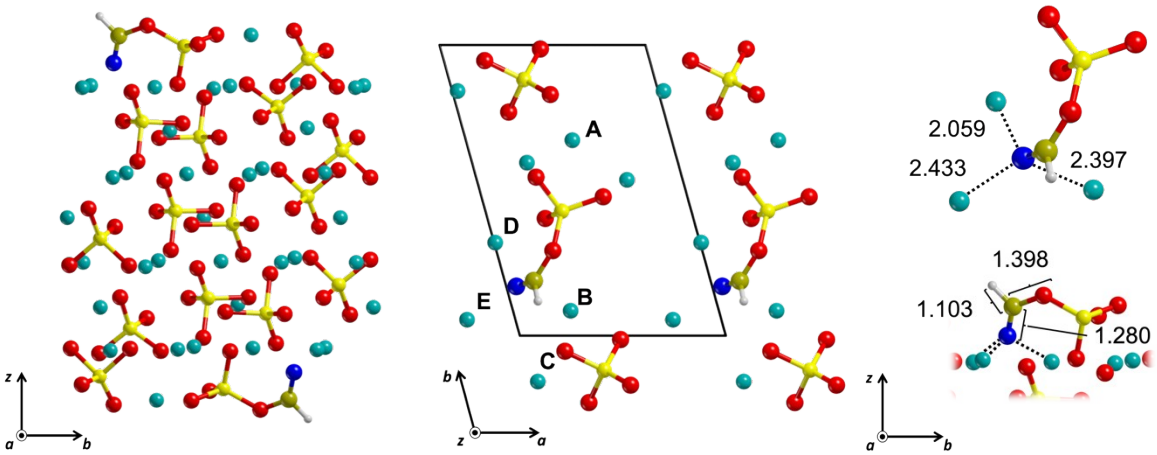

Figure S13. Side and top view of the (111) D structure. The same structure was obtained by placing the HCN molecule on the C and E sites.

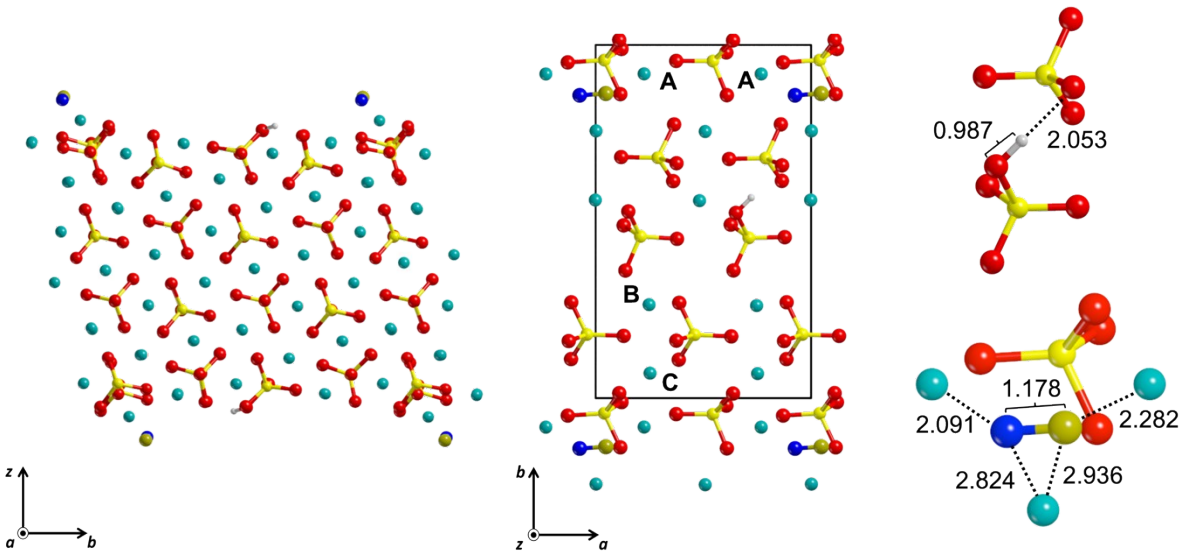

Figure S14. Side and top views of the (021) A structure.

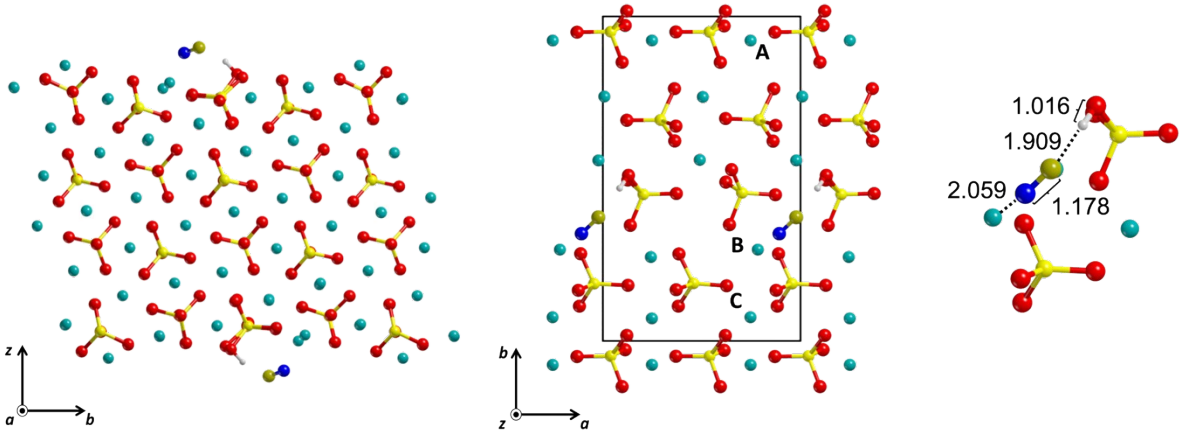

Figure S15. Side and top views of the (021) B_1 structure.

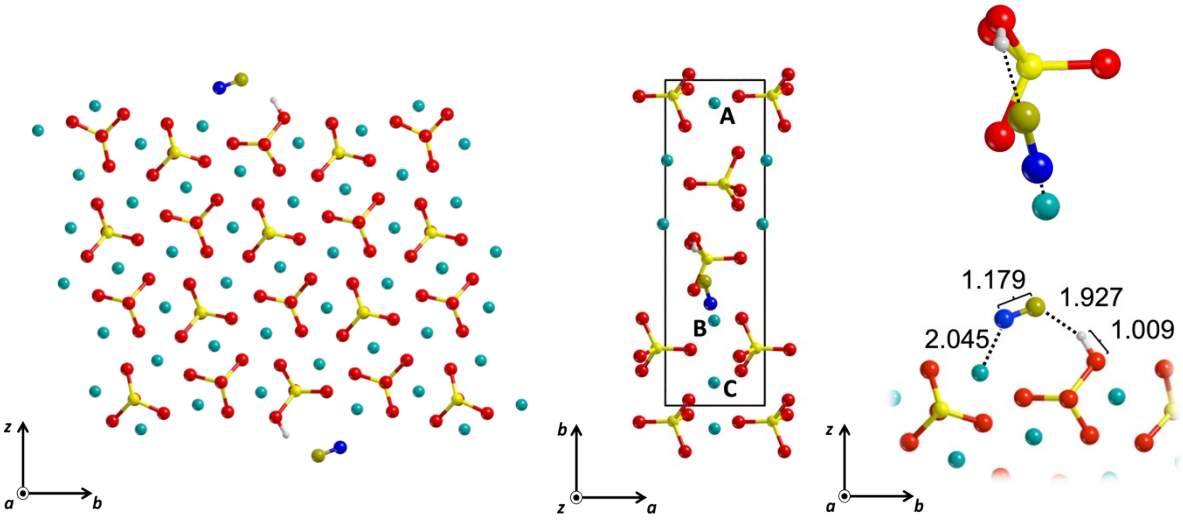

Figure S16. Side and top views of the (021) B_2 structure.

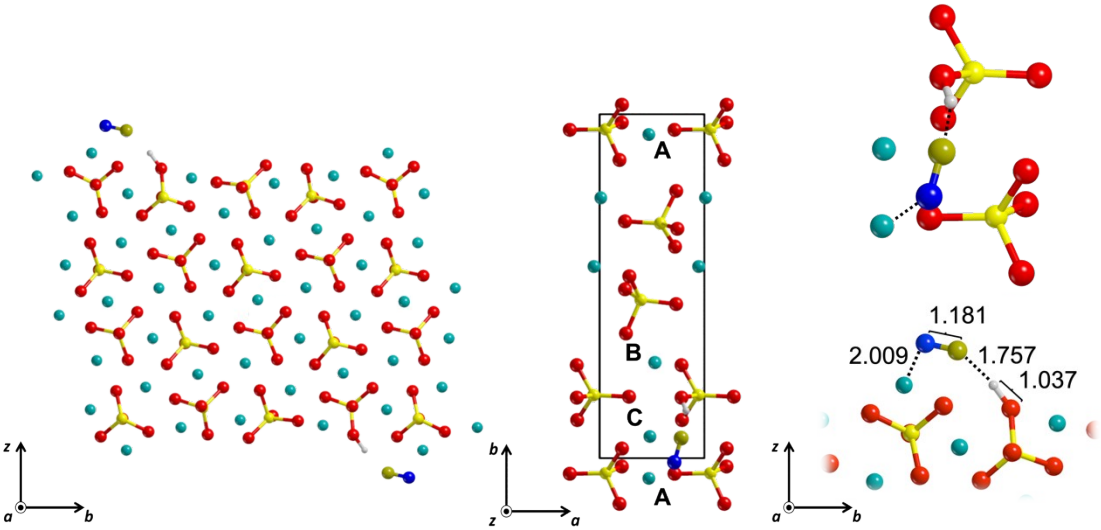

Figure S17. Side and top views of the (021) C structure. After initially placing the molecule on the C site, it displaced towards the A site during the geometry optimization.

Activated dissociation of adsorbed HCN molecules

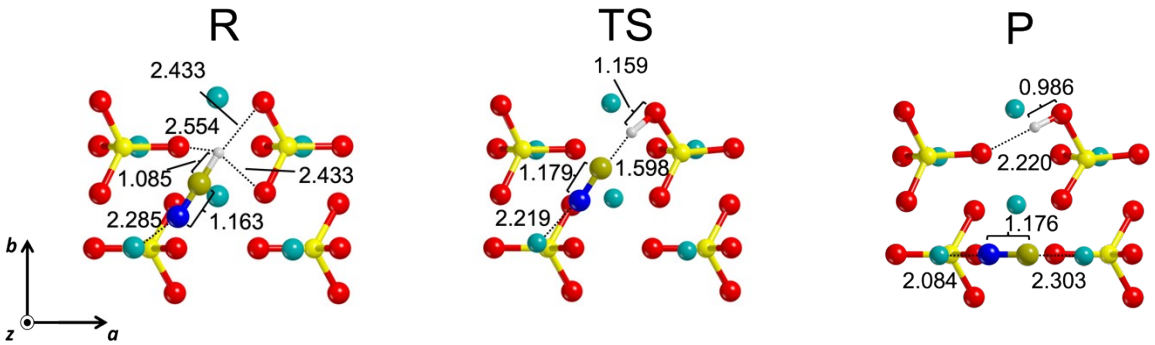

Figure S18. Reactant (R), transition state (TS) and product (P) for the activated dissociation taking place on the (010) A site.

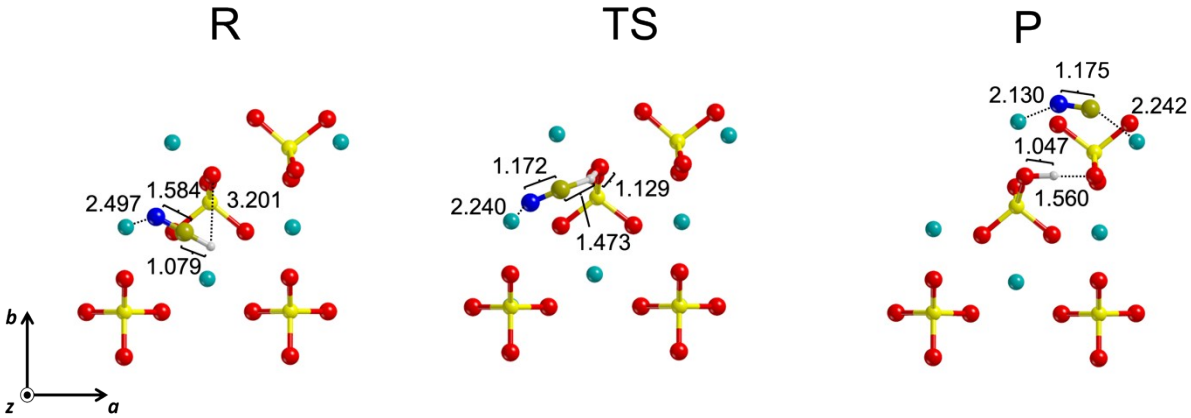

Figure S19. Reactant (R), transition state (TS) and product (P) for the activated dissociation taking place on the (120) B site.

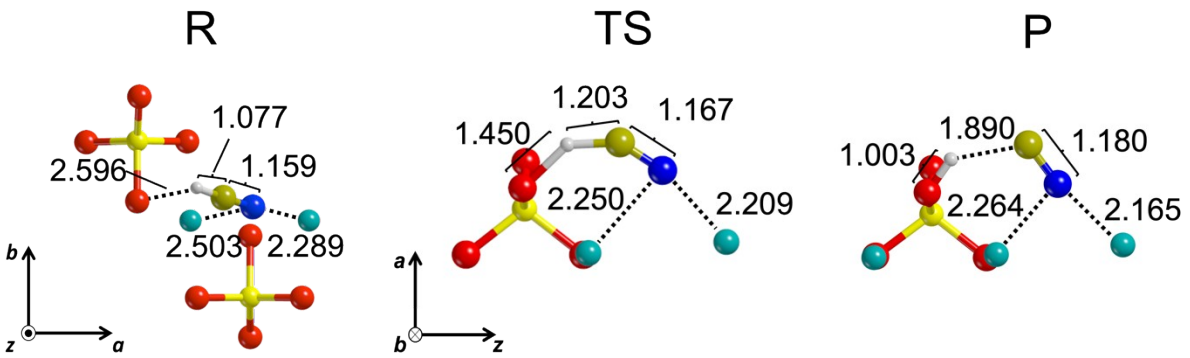

Figure S20. Reactant (R), transition state (TS) and product (P) for the activated dissociation taking place on the (120) C site.

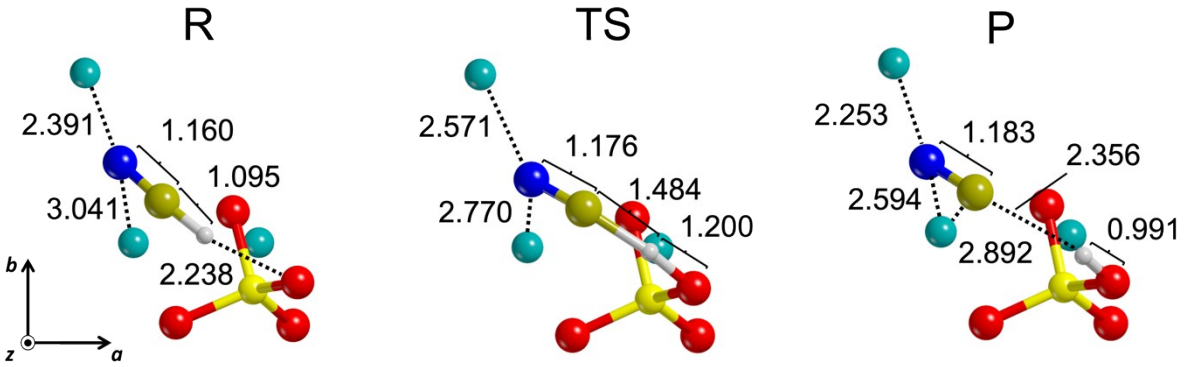

Figure S21. Reactant (R), transition state (TS) and product (P) for the activated dissociation taking place on the (101) B site.

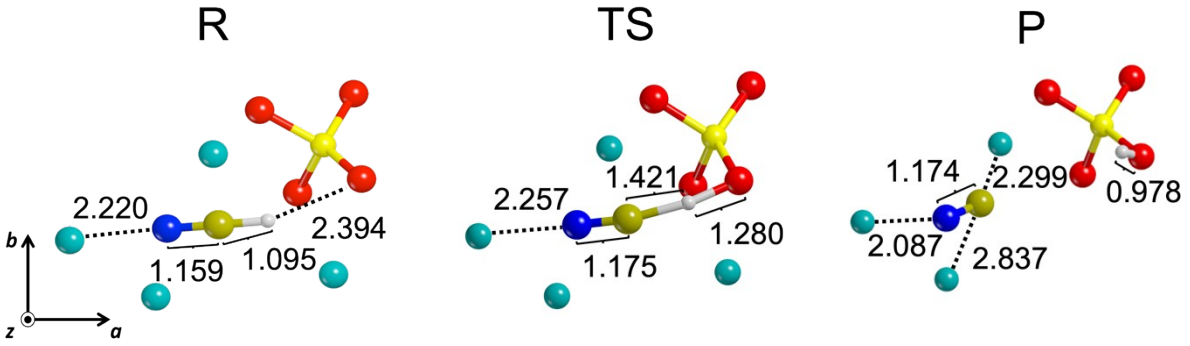

Figure S22. Reactant (R), transition state (TS) and product (P) for the activated dissociation taking place on the (111) A site.

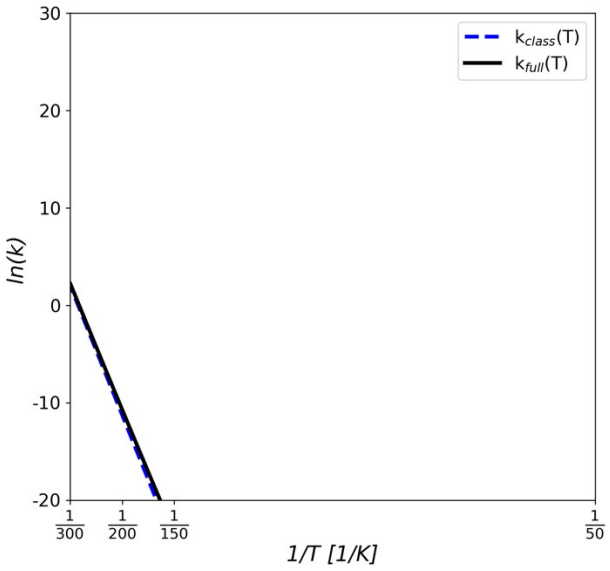

Figure S23. Calculated kinetic rate constants for the HCN dissociation from the (010) A adsorption complex. Arrhenius plot of k_{full} (black line) and k_{class} (blue dashed line) between 50 and 300 K. k units are in s^{-1}.

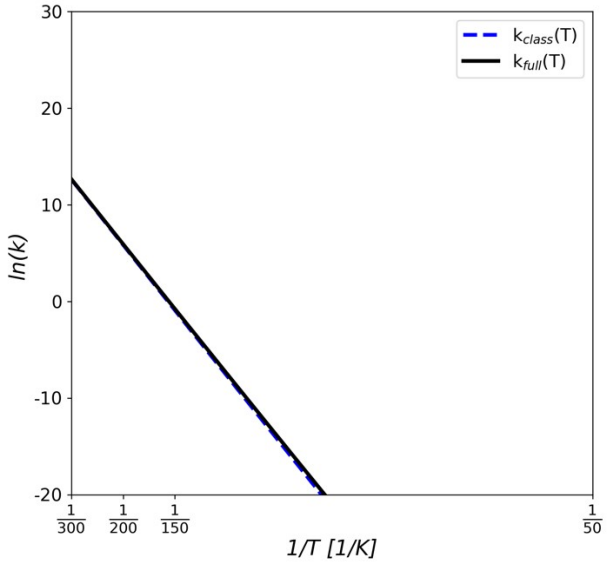

Figure S24. Calculated kinetic rate constants for the HCN dissociation from the (120) B adsorption complex. Arrhenius plot of k_{full} (black line) and k_{class} (blue dashed line) between 50 and 300 K. k units are in s^{-1}.

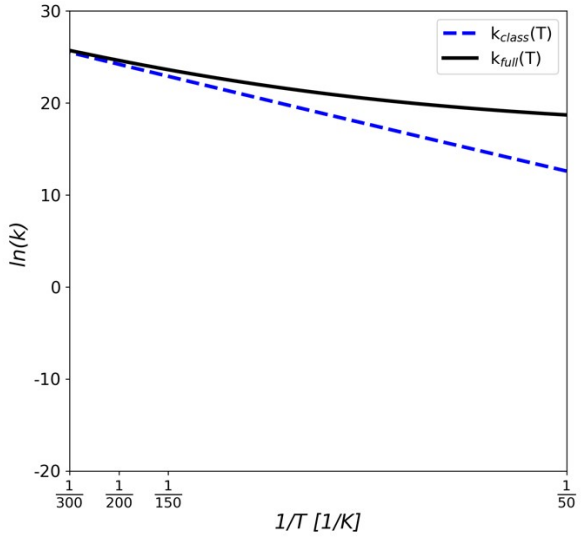

Figure S25. Calculated kinetic rate constants for the HCN dissociation from the (120) C adsorption complex. Arrhenius plot of k_{full} (black line) and k_{class} (blue dashed line) between 50 and 300 K. k units are in s^{-1}.

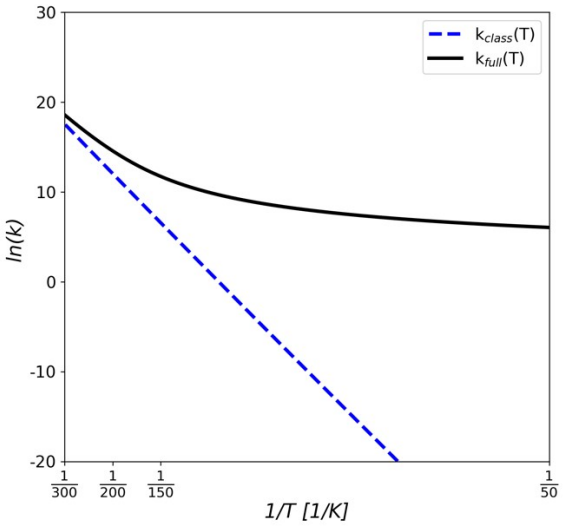

Figure S26. Calculated kinetic rate constants for the HCN dissociation from the (111) A adsorption complex. Arrhenius plot of k_{full} (black line) and k_{class} (blue dashed line) between 50 and 300 K. k units are in s^{-1}.

Table S1. Calculated rate constants excluding (k_{class}, s^{-1}) and including tunnelling effects (k_{full}, s^{-1}) and associated half-life times ($t_{1/2}$, s) for the HCN dissociation from different molecularly adsorption complexes considering different temperatures (T, K).

case	(010) A			(120) B			(120) C			(101) B			(111) A		
T	k_{full}	k_{class}	$t_{1/2}$	k_{full}	k_{class}	$t_{1/2}$	k_{full}	k_{class}	$t_{1/2}$ (s)	k_{full}	k_{class}	$t_{1/2}$ (s)	k_{full}	k_{class}	$t_{1/2}$
10	1.1e-45	<1.0e-300	6.6e+44	1.2e-58	1.3e-163	6.0e+57	2.6e+09	1.8e-02	2.7e-10	5.0e-04	1.2e-135	1.4e+03	1.3e+02	2.2e-117	5.5e-03
50	5.0e-34	4.3e-56	1.4e+33	3.9e-23	6.8e-24	1.8e+22	5.1e+10	2.0e+09	1.4e-11	2.8e-01	6.3e-18	2.4e+00	3.9e+03	2.2e-14	1.8e-04
150	2.3e-10	7.5e-11	3.0e+09	1.1e+00	9.3e-01	6.5e-01	3.1e+11	1.8e+11	2.2e-12	1.6e+04	5.4e+02	4.4e-05	7.2e+05	5.0e+03	9.6e-07
200	6.3e-05	3.6e-05	1.1e+04	7.5e+02	7.0e+02	9.2e-04	4.5e+11	3.1e+11	1.6e-12	9.1e+05	1.8e+05	7.7e-07	9.3e+06	7.8e+05	7.5e-08
300	2.2e+01	1.7e+01	3.1e-02	5.3e+05	5.1e+05	1.3e-06	6.6e+11	5.5e+11	1.1e-12	1.2e+08	6.3e+07	5.8e-09	3.4e+08	1.2e+08	2.0e-09

IR spectral features of adsorbed HCN molecules

Table S2. Structural and spectroscopic features of the 8 molecular adsorption cases (**M**). Second and third columns: computed stretching frequencies ($\bar{\nu}$), and bond lengths (d) and corresponding variations (Δ) for the C≡N and C-H bonds. Fourth: H-bond distances between the HCN and the oxygen atoms of the silicate surfaces. Fifth column: distance between the surface Mg^{2+} cations and the N-end of HCN. Last column: class to which the structure belongs according to the classification proposed in Figure 9. Frequencies are in cm^{-1} and distances in Å.

M	C≡N		C-H		O ⋯ HCN (H – bond)			Mg - NCH			
case	$\bar{\nu}$ (Δ)	d (Δ)	$\bar{\nu}$ (Δ)	d (Δ)	d			d_{Mg-N}			*Class*
(120) A	2019 (-78)	1.16001 (0.00031)	2702 (-609)	1.128 (0.052)	1.721	-	-	2.098	-	-	I
(010) A	2064 (-33)	1.16254 (0.00284)	3195 (-116)	1.085 (0.009)	2.309	2.433	2.554	2.185	-	-	I
(101) B	2076 (-21)	1.16051 (0.00081)	3081 (-230)	1.095 (0.019)	2.238	-	-	2.391	-	-	I
(111) A	2092 (-5)	1.15897 (-0.00073)	3088 (-223)	1.095 (0.019)	2.394	-	-	2.220	-	-	I
(120) C	2099 (2)	1.15933 (-0.00037)	3305 (-6)	1.077 (0.001)	2.596	-	-	2.289	2.503	-	II
(120) B	2099 (2)	1.15847 (-0.00123)	3276 (-35)	1.079 (0.003)	-	-	-	2.497	-	-	II
(001) B	2106 (9)	1.15802 (-0.00168)	3284 (-27)	1.078 (0.002)	2.446	2.726	2.845	2.173	-	-	II
(111) D	1526 (-571)	1.27994 (0.12024)	2942 (-369)	1.103 (0.027)	-	-	-	2.059	2.433	2.397	III

Table S3. Structural and spectroscopic features of the 8 spontaneous dissociative adsorptions (**D**) cases. Second column: computed stretching frequencies ($\bar{\nu}$) and bond lengths (d) and corresponding variations (Δ) for the C≡N bonds. Third column: computed stretching frequencies ($\bar{\nu}$) and bond lengths (d) for the O-H bonds. Fourth column: H-bond distances between the newly formed silanols and the acceptor atoms X, (X being either the C atom of a CN^- or the surface O atom). Fifth column: distance between the CN^- group and the surface Mg^{2+} cations, (d_{Mg-N} and d_{Mg-C}). Last column: class to which the structure belongs according to the classification proposed in Figure 9. Frequencies are in cm^{-1} and distances in Å.

D	C≡N		O - H		X ⋯ HO (H-bond)	Mg - CN					
case	$\bar{\nu}$ (Δ)	d (Δ)	$\bar{\nu}$	d	d (C/O)	d_{Mg-N}			d_{Mg-C}		*Class*
(111) B	1996 (-101)	1.18953 (0.02983)	3579	0.980	2.084 (C)	2.208	2.313	2.374	-	-	IV
(101) A	2053 (-44)	1.18186 (0.02216)	3026	1.009	1.849 (C)	2.008	-	-	-	-	V
(021) C	2061 (-36)	1.18094 (0.02124)	2585	1.037	1.757 (C)	2.009	-	-	-	-	V
(101) C	2039 (-58)	1.18504 (0.02534)	3521	0.986	2.071 (O)	2.129	2.317	-	2.747	-	VI
(021) B_2	2076 (-21)	1.17901 (0.01931)	3063	1.009	1.927 (C)	2.045	-	-	-	-	V
(021) A	2083 (-14)	1.17819 (0.01849)	3475	0.987	2.053 (O)	2.091	2.824	-	2.282	2.936	VIII
(021) B_1	2086 (-11)	1.17817 (0.01847)	2937	1.016	1.909 (C)	2.059	-	-	-	-	V
(001) A	2151 (54)	1.16972 (0.01002)	3752	0.972	-	2.078	-	-	2.127	-	VII

Table S4. Structural and spectroscopic features of the 5 manually dissociated (**MD**) cases. Second column: computed stretching frequencies ($\bar{\nu}$) and bond lengths (d) and corresponding variations (Δ) for the C≡N bonds. Third column: computed stretching frequencies ($\bar{\nu}$) and bond lengths (d) for the O-H bonds. Fourth column: H-bond distances between the newly formed silanols and the acceptor atoms X (X being either the C atom of a CN^- (C) or the surface O atom). Fifth column: distances between the CN^- group and the surface Mg^{2+} cations, (d_{Mg-N} and d_{Mg-C}). Last column: class to which the structure belongs according to the classification proposed in Figure 9. Frequencies are in cm^{-1} and distances in Å.

MD	C≡N		O - H		X ⋯ HO (H-bond)	Mg - CN				
case	$\bar{\nu}$ (Δ)	d (Δ)	$\bar{\nu}$	d	d (C/O)	d_{Mg-N}		d_{Mg-C}		*Class*
(010) A	2103 (6)	1.17573 (0.01603)	3497	0.986	2.220 (O)	2.084	-	2.303	-	VII
(120) B	2109 (12)	1.17458 (0.01488)	2496	1.047	1.560 (O)	2.130	-	2.242	-	VII
(120) C	2069 (-28)	1.17988 (0.02018)	3146	1.003	1.890 (C)	2.165	2.264	-	-	V
(101) B	2044 (-53)	1.18294 (0.02324)	3413	0.991	2.356 (C)	2.253	2.594	2.892	-	VI
(111) A	2114 (17)	1.17371 (0.01401)	3681	0.978	-	2.087	-	2.299	2.837	VII

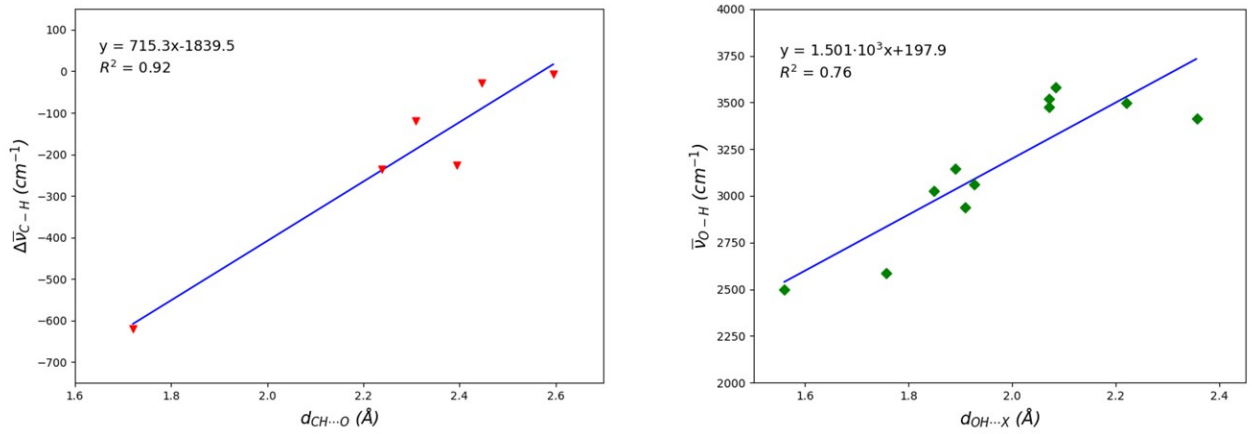

Figure S27. Left: dependence between the computed IR shifts ($\Delta\bar{\nu}_{C\text{-}H}$) and the corresponding hydrogen bond distances ($\Delta d_{CH\cdots O}$) for non-dissociative adsorptions. Right: dependence between the computed IR frequency ($\bar{\nu}_{O\text{-}H}$) and the corresponding hydrogen bond distance ($\Delta d_{CH\cdots X}$) for dissociative adsorptions. X represents either a C or another O atom.

References

1 M. Bruno, F. R. Massaro, M. Prencipe, R. Demichelis, M. De La Pierre and F. Nestola, Ab initio calculations of the main crystal surfaces of forsterite (Mg2SiO4): a preliminary study to understand the nature of geochemical processes at the olivine interface, *J. Phys. Chem. C*, 2014, **118**, 2498–2506.

2 A. Schäfer, H. Horn and R. Ahlrichs, Fully optimized contracted Gaussian basis sets for atoms Li to Kr, *J. Chem. Phys.*, 1992, **97**, 2571–2577.